



**STATISTICAL REMOVAL OF SHADOW
FOR APPLICATIONS TO GAIT RECOGNITION**

THESIS

Brian D. Hockersmith, Second Lieutenant, USAF
AFIT/GAM/ENC/08-04

**DEPARTMENT OF THE AIR FORCE
AIR UNIVERSITY**

AIR FORCE INSTITUTE OF TECHNOLOGY

Wright-Patterson Air Force Base, Ohio

APPROVED FOR PUBLIC RELEASE; DISTRIBUTION UNLIMITED

The views expressed in this thesis are those of the author and do not reflect the official policy or position of the United States Air Force, Department of Defense, or the U.S. Government.

**STATISTICAL REMOVAL OF SHADOW
FOR APPLICATIONS TO GAIT RECOGNITION**

THESIS

Presented to the Faculty of the
Department of Mathematics and Statistics
Graduate School of Engineering and Management
Air Force Institute of Technology
Air University
Air Education and Training Command
In Partial Fulfillment of the Requirements for the
Degree of Master of Science

Brian D. Hockersmith, B.S.
Second Lieutenant, USAF

March 2008

APPROVED FOR PUBLIC RELEASE; DISTRIBUTION UNLIMITED

**STATISTICAL REMOVAL OF SHADOW
FOR APPLICATIONS TO GAIT RECOGNITION**

Brian D. Hockersmith, B.S.
Second Lieutenant, USAF

Approved:

Samuel A. Wright, Maj, USAF
Thesis Advisor

Date

Kyle A. Novak, Maj, USAF
Committee Member

Date

David M. Kaziska, Maj, USAF
Committee Member

Date

Acknowledgments

First and foremost, I would like to thank my family. Regardless of the decisions I have made, their support and encouragement was always steadfast and without end. My wife has been a true hero in my life. She has aided me time and again through self-sacrifice and a never quit attitude. My parents are of particular importance; they never stopped believing in me and pushed me to become the person they knew I always could be. To my spouse's family, from the first day I met them, they embraced me with open arms and could always be counted on to offer support. Without the help and encouragement of all of these individuals, my dream to be the first person in my family to get a Master's Degree would never have come to fruition.

In addition, I would like to thank the instructors of AFIT for their guidance. In particular, I would like to thank Maj. Sam Wright for advising me on this thesis. His patience and insight brought the completion of this thesis into the realm of possibilities. I would also like to thank my committee members Maj. Kyle Novak and Maj. David Kaziska. To Maj. Kyle Novak, without your instruction on MATLAB, I never would have completed the manipulations needed to complete my thesis. It is my sincere thanks that I give to the Air Force for allowing me the opportunity to excel.

Table of Contents

	Page
Acknowledgments.....	iv
Table of Contents.....	v
List of Figures	vii
List of Tables	ix
Abstract.....	x
I. Introduction	1
Background	1
Problem Statement.....	1
Research Objectives.....	1
Research Question	2
Thesis Organization	2
II. Literature Review	4
Chapter Overview	4
Beginnings	4
Relevant Research.....	6
Processing Without Shadow Removal.....	8
Processing With Shadow Removal.....	9
Summary	11
III. Methodology	12
Chapter Overview	12
Data Collection	12
Research Step.....	12
Algorithms Developed.....	14
Hypothesis Test.....	16
Limitations	17
IV. Results and Analysis.....	19
Chapter Overview	19
Analysis of Test Data.....	19

Blue Background Analysis	20
Green Background Analysis	23
Red Background Analysis.....	25
Analysis of All Test Data.....	28
Implementation	37
Summary	41
 V. Conclusions and Recommendations	42
Chapter Overview	42
Conclusions of Research.....	42
Recommendations for Future Research.....	43
Summary	44
 Appendix A. MATLAB Algorithms.....	45
Function: Load Video	45
Function: Write Multiple Images.....	46
Function: Crop Images.....	47
Function: Three-Dimensional Data Plots.....	48
Function: Display Average RGB Intensities.....	49
Function: Computation of Three-Dimensional Distances	50
Function: Computation of Projected Three-Dimensional Distances	51
Function: Shadow Removal Algorithm	52
Function: Computation of Upper Confidence Intervals.....	54
Function: Computation of Coefficients for Shadow Removal Algorithm.....	55
Function: Plot of Rotation of Ellipsoid.....	56
Function: Shadow Removal and Back Ground Subtraction	57
 Bibliography	59
 Vita.....	61

List of Figures

	Page
Figure 1. True Binary Silhouette Algorithm.....	13
Figure 2. Blue Average Background and Typical Shaded Frame	20
Figure 3. Intensities of Average Blue Frame and Typical Shaded Blue Frame	21
Figure 4. Randomly Selected Pixel Values for the Blue Frames.....	22
Figure 5. Green Average Background and Typical Shaded Frame	23
Figure 6. Intensities of Average Green Frame and Typical Shaded Green Frame	24
Figure 7. Randomly Selected Pixel Values for the Green Frames	25
Figure 8. Red Average Background and Typical Shaded Frame.....	25
Figure 9. Intensities of Average Red Frame and Typical Shaded Red Frame.....	26
Figure 10. Randomly Selected Pixel Values for the Red Frames.....	27
Figure 11. RGB Histograms of Distances of Shaded Pixels to Centerline.....	30
Figure 12. 2D Plots of Projected Shadow Lines of Blue Background.....	32
Figure 13. 2D Plots of Projected Shadow Lines of Green Background	32
Figure 14. 2D Plots of Projected Shadow Lines of Red Background.....	32
Figure 15. Example of Ellipsoid Test Region.....	35
Figure 16. Representation of Transformations of Ellipsoid Test Region	37

Figure 17. Images Derived from Background Subtraction.....	38
Figure 18. Images After Ellipsoid Test and Background Subtraction.....	39
Figure 19. Images After Ellipsoid Test and Background Subtraction with Filter	40
Figure 20. Silhouette with Holes Filled	40

List of Tables

	Page
Table 1. Sample Pixel Values for Blue Background With Population Statistics.....	22
Table 2. Randomly Selected Pixel Values for Green Background.....	24
Table 3. Randomly Selected Pixel Values for the Red Frames	27
Table 4. Two-Dimensional Distances of Shadow Pixels to Ellipsoid Centerline.....	31
Table 5. Average Distances of First Ten Shaded Frames.....	33
Table 6. Upper Confidence Intervals	33

Abstract

The purpose of this thesis is to mathematically remove the shadow of an individual on video. The removal of the shadow will aid in the rendering of higher quality binary silhouettes than previously allowed. These silhouettes will allow researchers studying gait recognition to work with silhouettes unhindered by unrelated data.

The thesis begins with the analysis of videos of solid colored backgrounds. A formulation of the effect of shadow on specified colors will aid in the derivation of a hypothesis test to remove an individual's shadow. Video of an individual walking normally, perpendicular to the camera will be utilized to test the algorithm.

First, the algorithm replaces shaded pixels, pixel values determined to be shadows, with corresponding pixels of an average background. A hypothesis test will be employed to determine if a pixel value is a shaded pixel. The rejection region for the hypothesis test will be determined from the pixel values of the frames containing a subject.

Once the shaded pixels are replaced, the resulting frames will then be run through a background subtraction algorithm and filtered, resulting in a series of binary silhouettes. Researchers can then utilize the series of binary silhouettes to accomplish a gait recognition algorithm.

STATISTICAL REMOVAL OF SHADOW

FOR APPLICATIONS TO GAIT RECOGNITION

I. Introduction

Background

All individuals possess a trait that is identified as the human gait. Several aspects of the motion of natural walking can be decomposed into useful mathematical data. Examples of these motions are the length of a stride, the angle of a bended knee, the height of an individual, the angle between two legs at maximum angle apart, et cetera. This information is extractable in lab conditions or in real life settings with the proper equipment and set-up. In addition, the subject does not have to give consent to the surveillance. Individuals are constantly observed by cameras with or without their consent. This occurs on a daily basis through traffic, automated teller machines, and security cameras.

Problem Statement

To utilize recorded video of individuals walking at a 90-degree angle to a fixed camera position and remove the shadow the individual projects on surfaces, such as the ground, without losing a significant amount of data related to the individual.

Research Objectives

The objective of this thesis is to find the relationship between colors and their shaded counterparts. Once this relationship is derived mathematically, the algorithm will

remove shaded colors. The algorithm needs to be concise to eliminate errors in processing and broad enough to remove as many shadow pixels as possible without compromising the integrity of the data. The algorithm will then be employed on prerecorded video of an individual walking.

The shadow pixel removal will ensure noise reduction from the video before a background subtraction method is utilized. After the shadow and background subtraction has been accomplished, the resulting binary image needs smoothing to reduce errors in processing. The smoothing will involve algorithms pre-built in MATLAB.

The algorithms will take prerecorded video of an individual walking and extract a mathematical representation of the individual depicted in the video. In addition, the constructs derived are written so they do not require human interaction. Every program, once initiated, runs without the input of parameters, except the images themselves.

Research Question

Is it possible to derive an algorithm to remove shadow from a video feed without compromising the integrity of objects to be observed?

Thesis Organization

The second chapter discusses the accomplishments and theories of individuals working on similar research. The ideas discussed illustrate the level of exploration that researchers have put forth in this area of gait biometrics. In addition, the beginnings of gait biometrics and practical uses are communicated. The discussion will center on the work done by researchers in the area of noise removal, such as shadow or background.

Their algorithms to accomplish gait recognition will be briefly highlighted to illustrate their common need to remove noise in the data.

The third chapter illustrates the methodology employed. The collection of data will be thoroughly discussed. Explanations of all MATLAB algorithms employed to reach conclusions in Appendix A will be included. In addition, contained in the chapter are limitations of the hypothesis test and the methods utilized to derive conclusions. The hypothesis tests to determine shadow pixel feasibility will be incorporated in the third chapter.

The fourth chapter contains the results and analysis of the data processed. Discussions of the mathematical formulas utilized to derive the MATLAB algorithms are also contained in the chapter. Pictorial representations of the data are plotted in three dimensions to aid in the visualization of the properties of the backgrounds and the shaded pixels.

The fifth chapter contains conclusions derived from the analysis of data. In addition, recommendations for further research are discussed. Finally, there will be a summary of findings.

II. Literature Review

Chapter Overview

This chapter is dedicated to the past research accomplished in the field of gait decomposition. The primary focus deals with the findings of scientists related to processes for useable data extracted from video feeds of individuals. Researchers employ varying methods for gait recognition depending on particular self imposed extraction methods.

“Human movement analysis aims at gathering quantitative information about the mechanics of the musculo-skeletal system during the execution of a motor task” (Cappozzo, 2006:186). In addition, Merriam-Webster’s online dictionary describes biometrics as “the measurement and analysis of unique physical or behavioral characteristics (as fingerprint or voice patterns) especially as a means of verifying personal identity” (“Biometrics,” 2007). Biometrics, in regards to the human gait, has been used in the past for medical and gait recognition research.

“All humans follow the same basic walking pattern, but their gaits are influence[d] by functions of their entire musculo-skeletal structure” (Post, 2006:1). The individuality of walking patterns are derived in part from height, weight, build, injuries, shoes, and stress. Some gait attributes vary from day to day. Objects like briefcases and backpacks hinder researchers’ abilities to distinguish individual’s biometrics.

Beginnings

The human gait can be broken down into components. An online medical dictionary states the human gait can be broken into three phases. One phase is the “stance phase” where both feet are holding the weight of the person. The “swing phase”

refers to the time when a person has all of their weight on one foot and the other is suspended in the off of the ground. The third phase is an inverted swing phase, where the opposite foot supports the weight (“Gait,” 2007).

The medical community has long utilized the analysis of gait to determine muscular or skeletal problems with patients. A conjunction of several different systems can be used to obtain data about a specific gait trial. “Cameras, magnetic fields, electromyography (EMG) data, and force plates are all methods for used for data collection” (Post, 2006:6). These items normally record a person’s gait biometric under laboratory conditions. These processes seek to eliminate noise derived from parameters not associated with the individual included in the data feed.

This type of data collection involves the collaboration of the patient. Researchers have the ability to record massive amounts of data about any one facet or a whole multitude of parameters involved with an individual’s gait biometrics (Post, 2006:5). With the data obtained, doctors and technicians can recommend a particular treatment or pinpoint a problem. These types of problems originate from sports injuries, strokes or a multitude of other factors. With aid of computer-based gait data, therapists can measure progress mathematically, thereby reducing the human error. This human error can come from the constant repetitive treatments required by patients to return to normal gait (Post, 2006:8).

The medical community has almost limitless access to a volunteered patient. The patients are self-motivated to give medical professionals full access to help remedy their particular medical condition. However, researchers in the gait recognition field utilizing field video data generally have seconds to record data under non-ideal conditions.

Relevant Research

Non-ideal conditions constitute a noise that analysts in the field must deal with. Isolated feature extraction is an integral part of gait decomposition. Data extracted with less noise would be more useful to researchers. Several concerns arise from data collected in the field. All subjects walking in captured video will appear at varying lengths from the camera. The process should scale the image accordingly (Boulgouris, 2006:971). As an individual crosses the frame of reference for the camera, their placement in the frame shifts frame right to left or left to right. A gait detection algorithm should account for frame alignment (Boulgouris, 2006:971). If a background subtraction is utilized, the algorithm should correct for imperfect background subtraction. In addition, even with the advent of faster and faster computers, the process should require low computational power (Boulgouris, 2006:971). These areas of concern surround the building of general algorithms, however, they do not limit the means to identify individuals through mathematical interpretations of data captured from video surveillance.

The methods of biometric gait identification can be divided into 2 categories, model-based and motion-based (Post, 2006:2). When researchers take a predetermined composite and then match new data to it that is a model-based approach (Post, 2006:2). Extrapolating information from a subject and analyzing it equates itself to a motion-based approach (Post, 2006:3). Both approaches seek the ability to categorize and compare sets of unrelated data.

Model-based approaches neglect to account for irregularities in gait (Foster, 2003:2490). These irregularities include the subject carrying a briefcase or a backpack.

One way a model-based approach could account for irregularities is if a database was created for each type (Foster, 2003:2490). Of course, there would be a multitude of irregularities to consider. Moreover, a database for each irregularity would need to be as extensive as the normal gait database. This type of approach is usually mathematically intricate (Foster, 2003:2490).

Motion-based approaches try to remove the human element from the equation. Using this approach, researchers utilize a binary silhouette or some other shape representation to extract data. The extraction can be done through the motion created by the object or direct matching with a database of silhouettes (Post, 2006:3).

Both approaches deal with similar problems. Researchers determine which variables are noise related and need to be removed before classifications are done. The issue of shadows derived from the individual subject is one source of noise, so shadow removal is the major goal of this thesis. Shadows normally obstruct leg movement, depending on sun placement. The darkness of the shadow also varies with light intensity. The shadows from moving clouds will also add noise to the data. Several papers have approaches to deal with the problems associated with this noise and then compare individual biometrics to those in a database.

The researchers that derived biometric comparison algorithms are of particular importance to gait recognition analysts. This research works towards the decomposition of biometrics for use in a later recognition program. Nonetheless, a brief description of methods used to facilitate these comparisons will be discussed.

Processing Without Shadow Removal

Before gait comparison algorithms can be employed, the separation of individuals from their background is an initial goal that gait recognition algorithms generally seek to obtain. Through a technique dubbed “non-linear point distribution model,” researchers extracted the motion of the human form from video of a moving subject (Bowden, 2000:729). Researchers were able to create a body contour using an individual’s outstretched hands and head (Bowden, 2000:731). The process was accomplished via a blue screen and chroma keying (Bowden, 2000:732). This technique is similar to how the backdrop of a television weatherman is made to appear to be constantly changing. This process worked well in laboratory conditions, shadow was not a factor.

Researchers from The Hong Kong Polytechnic University avoided the removal of shadow through the incorporation of “motion silhouette contour templates (MSCTs) and static silhouette templates (SSTs)” (Lam, 2006:2563). The silhouettes obtained for this gait comparison algorithm included shadows. The images were scaled to 128 by 88 pixels to account for the different sizes of the silhouettes (Lam, 2006:2566). The MSCTs generated from the data are representations of one individual’s gait cycle (Lam, 2006:2567). The SSTs are a means to exclude errors in comparisons of gait (Lam, 2006:2569). A background subtraction method was accomplished to render silhouettes in this process. The gait recognition process yielded successful matches 80 percent of the time (Lam, 2006:2563).

An additional technique for automatic gait analysis involves “masking functions to measure area as a time varying signal from a sequence of silhouettes of a walking subject” (Foster, 2003:2489). In order to get silhouettes into a state that is feasible for

this type of analysis, the silhouettes need to be processed. The process employed begins with a background removal algorithm. Since data was collected in laboratory conditions, a solid backdrop was used and the silhouette was extracted through a chroma-key technique (Foster, 2003:2491). The researchers then cropped the pieces of the image above the walking subject and the solid backdrop. The final images were scaled to a 64 by 64 pixel box to account for distance from the camera (Foster, 2003:2491). The final data obtained for comparison was derived from horizontal and vertical masks isolating particular body segments (Foster, 2003:2492). With the use of laboratory conditions researchers in this experiment avoided the problem of shadow removal.

Processing With Shadow Removal

Shadow pixels are classified as the shadow cast by the object on surfaces or the shadow projected onto the object itself (Wang, 2004:649). Researchers work with shaded pixels in a variety of ways. Another gait decomposition algorithm utilizes manually constructed silhouettes where components are weighted to accomplish gait style matching (Boulgouris, 2007:1766). The components are comprised of the arms, thighs, legs, lower torso, and head. This method resulted in a relatively high match percentage. Researchers were able to match a prior subject's gait cycle to a later recorded gait cycle. This algorithm was accomplished after silhouettes were manually derived from data and were scaled to account for the varying heights of individuals (Boulgouris, 2007:1764). Although the researchers removed the shadow, the process was done manually which requires to many man-hours to be practical. The binary silhouettes were derived from the University of South Florida Human Identification Gait Challenge data.

University of South Florida Gait Challenge data is a database of “300 GB (gigabytes) of data related to 452 sequences from 74 subjects” (Phillips, 2006:137). The purpose of the experiment was to create a massive database to allow researchers to incorporate their respective algorithms utilizing a common data set. Some of the 74 individuals were recorded inside, outside, and on different days using different perspectives and wearing different clothes (Phillips, 2006:137). The images were processed using a background subtraction method similar to those previously discussed in research. The binary images were cleaned up using a 9 by 9 pyramidal averaging filter (Phillips, 2006:137). Boxes were manually assigned to the silhouettes to remove unnecessary data. The researcher’s algorithm worked well when the factors of surface and shoe type were mitigated. Shadow removal was accomplished through a combination of manual procedures for the bounding of a subject and automatic filtering.

One approach to automatically remove a subject’s shadow employs an “eigen-stance” gait model (Liu, 2005:170). Each ordered frame of a recorded gait is projected into a subspace created by a Hidden Markov Model (Liu, 2005:173). A new silhouette is created with the original silhouette data “projected onto the matched eigen-stance model” (Liu, 2005:173). The method of background subtraction made use of “Gaussian statistical models” (Liu, 2005:173). Researchers calculated the red, blue, and green (RGB) data of each pixel to include mean and variance. Utilizing the mean and variance information the researcher’s algorithm determined whether a pixel was background or not. This process works quite well with the absence of dark shadows. The projections and preloaded body shapes allowed researchers to remove shadow leaving a silhouette comprised entirely of body components.

Summary

The researchers presented in this chapter incorporated several varied ways to a subject from the surrounding background. The motive for their research centered on the final objective of gait recognition. Many utilized background subtraction algorithms and processed the silhouettes according to the requirements of their algorithms. Some researchers set their test subjects in blue screen rooms or ideal laboratory conditions to mitigate the outside influence of variables like shadow. Methods for dealing with shadow removal ranged from manual deletion to incorporation into the researchers' respective algorithms. This thesis attempts to automate the process of shadow removal so that the entire process of gait recognition may be likewise automated from the capture of video to individual discrimination.

III. Methodology

Chapter Overview

In this chapter, descriptions of practices taken to collect data for this thesis are discussed. The problem of isolating the human gait comes with the problem of isolating human gait from the background. When background subtraction is performed, the human gait as well as the shadow of the individual typically remains in each frame. Therefore, a methodology for removing shadows is presented. Furthermore, all MATLAB algorithms utilized to derive results are discussed. Finally, limitations associated with the algorithms and processing are conveyed.

Data Collection

The test data collected for processing originated with the filming of three test backgrounds. Filming was accomplished at 10:30 a.m. to diminish morning haze and allow for longer shadows. Cloud cover was minimal. The camera in this experiment was locked onto a tripod located 54.5 inches above the ground to minimize camera shake.

Three different solid colored 18 by 12 inch construction paper sheets were placed horizontally on a concrete surface and filmed in open sunlight and under shadow. An opaque plastic can was placed between the construction paper and the sun to produce shadow. Several seconds of video were captured of each color background under both sun light and shadow conditions

Research Step

Researchers have dealt with the removal of shadows in silhouettes in several ways. The manual removal of shadow runs the risk of removing pertinent data and is left

to an individual's interpretation of the data. The time needed to accomplish a manual rendering of shadow removal makes it impractical to employ. Alternatively, some researchers choose to incorporate noise left after imperfect background subtraction methods into their algorithms. This thesis will develop and demonstrate an effective automated removal of shadow and will further show the removal of shadow may be accomplished before a background subtraction algorithm is used. The process is described in Figure 1.

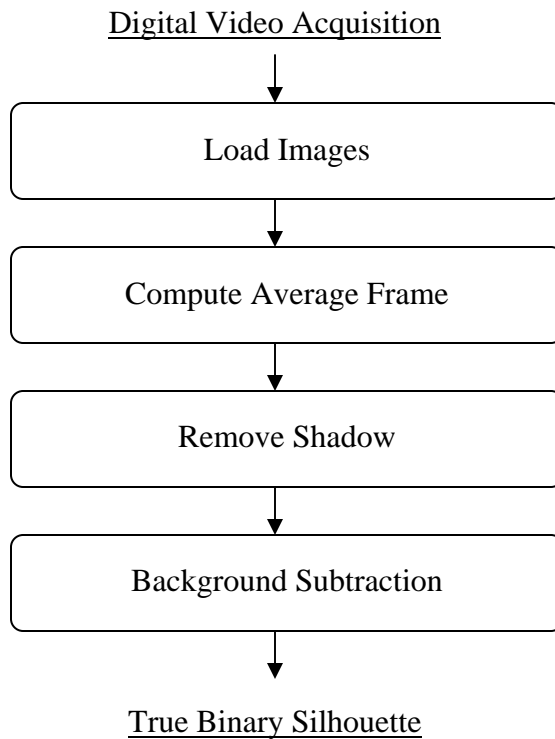


Figure 1. True Binary Silhouette Algorithm

The first step taken in the desire to remove shadows was to determine the effect of shadow on each of the three dimensions of color. Images are represented by varying degrees of red, green, and blue (RGB). Red, green, and blue backgrounds were chosen

because these are the colors whose intensities, relative and absolute, are represented by positive integers up to 255. By testing the effects of shadow on specific pixels located in the solid backgrounds, the effect of shadow can be derived for different pixel value combinations.

Solid colors were utilized as a background in order to remove as many variables as possible from the experiment. A researcher taking an average background would have to account for the movement of the camera and the blending of colors with a multicolored background. Pixels with wide variations in color may reside next to each other giving skewed results. The separate analyses of these three solid backgrounds showed a correlation utilized to predict the effect of shadow in a multitude of situations.

Algorithms Developed

In order to extract the data necessary to perform the analyses, several MATLAB algorithms were employed. The frames were extracted from video using the MATLAB function LoadVideo that is located in Appendix A. The image array is then saved to the computer with an algorithm similar to Writemulti located in Appendix A. At least 30 frames of 480 by 720 pixels of the sunlight-covered solid colored construction paper were recorded. Over 100 frames of solid background completely covered in shadow were recorded. Frames with the shadow partially covering the background were removed. The images were then cropped to 100 by 200 pixels with the function Crop in Appendix A. This was done to remove everything except the solid colored construction paper from the test region. The function Crop also writes the cropped image to file.

Once the images were cropped and saved, the data was processed. To facilitate the visualization of the data represented in this thesis, several algorithms were

constructed. The function DataPlots constructs a three-dimensional plot of the pixel values of the average background and the average pixel values of shaded frames. The function RotationPlot illustrates the effect of rotation matrices on a line and the ellipsoidal rejection region of the hypothesis test. RGBBackground is an algorithm designed to illustrate the level of intensities of the three components of a picture (Samler, 2006:60). These algorithms display the properties of data acquired and computational algorithms are discussed next.

Computational algorithms were derived to statistically analyze the data. The average distances of shaded pixels from a predetermined line are computed via the algorithm DistanceValues. The algorithm DistanceProjectedValues outputs the distances of a projected line to a point on a predetermined line. The 95 percent upper confidence intervals of the distances are computed with the function Confid. The algorithm Coeff outputs the coefficients utilized in the shadow removal algorithm. The bases of these algorithms will be discussed in Chapter IV.

Once the outputs were derived from the computational algorithms, these outputs were incorporated into an algorithm for shadow removal. In order to accomplish the shadow removal, an average background of sunlight-covered background is determined via MATLAB. This average background is incorporated into several algorithms. Once the average background is derived, the algorithm will then derive an ellipsoidal test region. If the values of a pixel are found to lie in the interior of the ellipsoid, the specific pixel will be replaced with the value of the corresponding pixel in the average picture. The MATLAB code ShadowTest is employed on the test data to remove shaded pixels. This code will be discussed in detail in the Chapter IV. Since the shadow removal

algorithm was built to accommodate any background, it is capable of performing the same process on other video data.

Hypothesis Test

A hypothesis test is utilized to accomplish shadow removal. The effect of the presence of a shadow on a particular pixel is that the representative values in the RGB primary colors are lowered. This is due to the fact that lower relative numbers represent darker colors. The lowering of the values of each of the RGB components is dependent on the relationship between each of the RGB components. For example, if the RGB components are relatively equal, shaded pixels follow a relatively or approaching linear path towards the origin. If the RGB components are not relatively equal, the shaded pixels are found to be contained in an ellipsoid whose center is a linear path to the origin from the original pixel value. The relationship between the RGB values of shaded pixels dictates the size and shape of an ellipsoidal rejection region. If a pixel value resides in the ellipsoidal region, it is considered shadow and is replaced with the corresponding pixel values from the average background.

The dimensions of the ellipsoidal rejection region will be derived from the pixel values of each frame to be tested. The major axis of the ellipsoid comes from the distance of a pixel value in RGB coordinates to the origin. The two minor axes are also derived from the RGB values of the pixels.

The height of the ellipsoid is derived from the combination of blue/red or blue/green components. The width of the test area corresponds to the green/red component pixel values. The derivation of the formula to achieve the correct height and width of the ellipsoid is discussed in detail in Chapter IV.

The ellipsoidal area represents the rejection region. The null hypothesis of the hypothesis test is the statement, “The pixel value is a shadow pixel.” The alternative hypothesis is, “The pixel value is not a shadow pixel.” If a particular pixel value of the frame were found to be a shadow pixel, it is replaced with the corresponding pixel from the average background. If the pixel is not a shadow pixel, it is unchanged.

Limitations

Inherent in all hypothesis tests is the possible misclassification of tested data. Three such misclassifications are considered. First, the hypothesis test can deem background pixels as shaded pixels. If this error occurs, the background pixel is replaced with the average background pixel. This type of error does not result in any loss of pertinent data.

Second, the hypothesis test can identify part of the individual as a shaded pixel. If this type of error occurs the result would be a loss of data needed to create a binary silhouette. This type of error would occur if the pixel value of the person’s hair, skin, or clothing resided in the ellipsoid test region. Small holes in the silhouette can be remedied with built-in MATLAB functions. In contrast, large cuts in the silhouette have little chance of remediation without manual intervention.

Third, it is possible for the value of a shadow pixel to be deemed a non-shadow pixel. This type of error would occur if the natural variation in a pixel’s RGB values placed it outside the ellipsoidal rejection region. If the number of unreplace shadow pixels is sufficiently low, built-in smoothing functions in MATLAB may remove the small percentage of errors.

Other types of errors are inherent to the algorithms employed. If a background contains moving objects, these objects may be identified as silhouettes. For example, a video of a crowded street may not be an ideal setting. In addition, a person walking in the opposite direction of the intended target poses a difficult problem to a background subtraction method.

Furthermore, the ellipsoidal rejection region utilized for the hypothesis test is derived from two rotation matrices. If the coordinates of a pixel lie along two of the three axes, gimbal lock may occur. This refers to the problem of when the two rotation matrices approach 90 degrees; the third axis cannot be accounted for or changed. This error is deemed unlikely, however, since on nearly all real world situations, color is composed, to some degree, of all three considered colors, red, green, and blue.

The limitations of the hypothesis test are complicated by the limitations of the camera utilized for data collection. The number of pixels recorded by the camera for each frame is directly correlated to the quality of the resulting silhouettes. In addition, the ability of the camera to accurately interpret its usual field of view is imperative to silhouette resolution.

IV. Results and Analysis

Chapter Overview

This chapter will examine the analysis and results obtained through research of frames of three solid colored backgrounds, as well as frames of actual gait data. In order to deconstruct an individual's gait, elements of the video other than the individual studied need to be removed. This includes the visible background and shadow produced from the blockage of light. Previous work has successfully removed the background with some residual noise in the data. Here is presented a viable methodology to remove the shadow using the test data of three solid colored backgrounds. The method is then implemented on video data containing an individual walking perpendicular to the camera (Samler, 2006:27). This data will be referred to as gait data. The test data of the three solid colored backgrounds was collected by the current researcher while the gait data of individuals walking across the frame was collected by Samler (Samler, 2006:27).

Analysis of Test Data

Test data was recorded on a day when conditions were optimal for an unobstructed view of the sun. Recordings were accomplished when the shadow was of a size adequate to completely cover the solid background material. In addition, in order to minimize the effect of uncontrollable shadow fluctuations, recording was accomplished when clouds were sparse.

Minimized environmental conditions are one aspect of the controlled experiment. Solid backgrounds will constitute another aspect of the controlled experiment. The three colors of the solid backgrounds were red, green, and blue. They were chosen because joint photographic experts group (jpeg) files are stored in a RGB format. Individual

frames were stored to computer in a jpeg format utilizing MATLAB. Each frame of data was stored in a 480 by 720 by 3 format. This relates to three 480 by 720 pixel frames representing the RGB colors. The 450 test data frames collected were cropped to 100 by 200 in order to contain the maximum amount of solid background. Each of the red, blue, and green backgrounds is analyzed separately, and the results are used to drive a hypothesis test to effect the removal in the gait data.

Blue Background Analysis

The results from the 150 blue background frames are analyzed first. Due to minor variability in the pixel values, it is more feasible to work with the average of several frames without shadow visible. This variability may be the result of ripples in the construction paper or camera shift. Therefore comparisons of shadow covered individual frames will be done with the average sunlit frame. After these images were recorded, a solid object was placed between the sunlight and the construction material. Further video was recorded with a shadow covering the blue background. The average blue background of the first twenty frames and a typical shaded frame is shown in Figure 2.

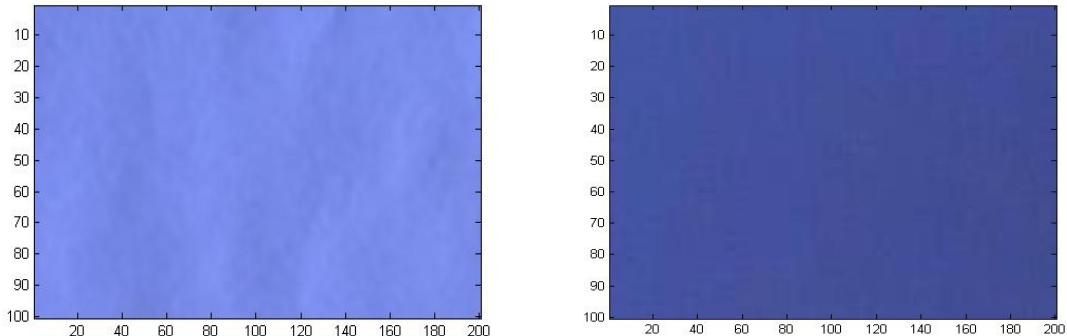


Figure 2. Blue Average Background and Typical Shaded Frame

Figure 3 displays the average individual RGB intensities of the blue average background and a typical shaded frame. The smallest average pixel value represents the least intense color. Since the figure depicts a strictly blue background, the tallest bar in each chart corresponds to the blue component. The background color is visually affected by the introduction of shadow. In addition, the intensities of the average RGB components are lessened by the introduction of shading.

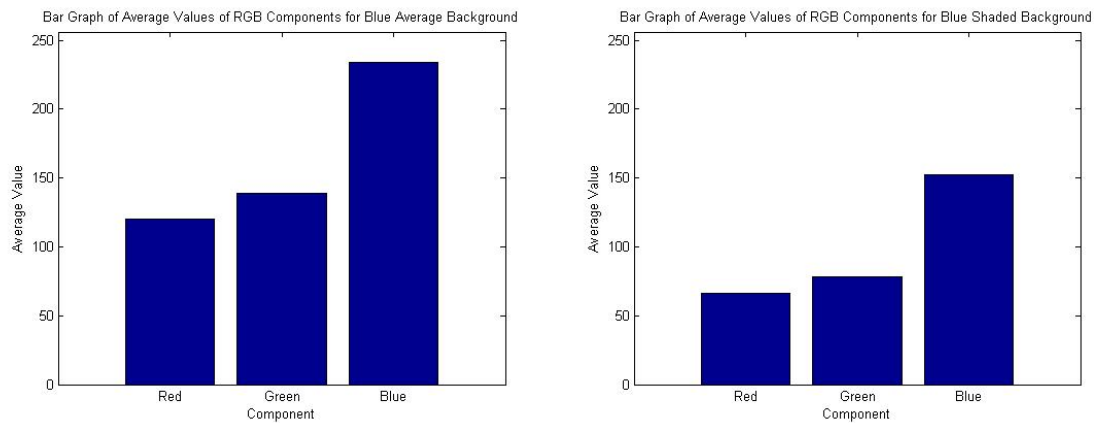


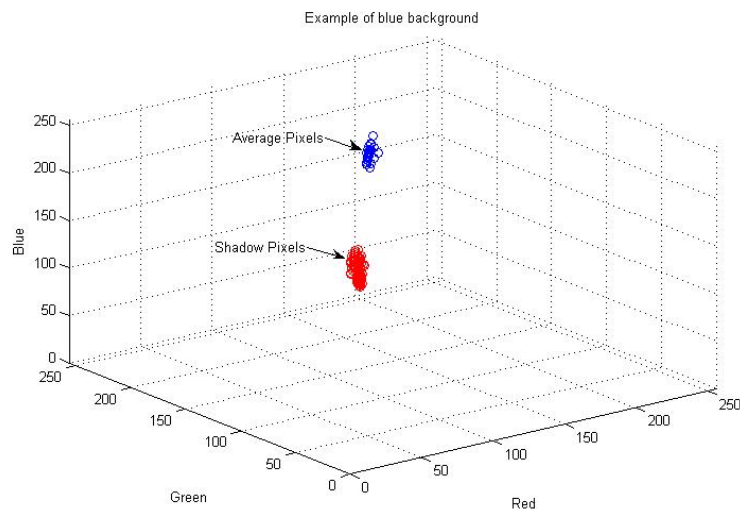
Figure 3. Intensities of Average Blue Frame and Typical Shaded Blue Frame

Table 1 displays pixel values in the RGB spectrum for 10 randomly selected pixels. It is shown that the intensities of each of these RGB component pixel values are significantly reduced. This is due to the level of the shadow and the placement of the original average pixel without shadow. Intuitively, the darker the shadow, the closer a pixel's value approaches (0,0,0). The mean and standard deviation are derived from the entire population.

Table 1. Sample Pixel Values for Blue Background With Population Statistics

	Red Component		Green Component		Blue Component	
	No Shadow	Shadow	No Shadow	Shadow	No Shadow	Shadow
112	70	130	79	224	154	
116	65	135	82	230	160	
125	66	144	78	242	154	
116	62	136	73	231	139	
120	65	139	78	235	148	
122	65	141	74	236	143	
120	67	140	80	235	159	
118	69	136	79	230	164	
121	70	139	82	234	164	
121	72	141	85	238	164	
Mean	120.63	67.54	139.53	80.60	234.91	156.65
St. Dev.	1.63	0.33	1.74	0.36	2.32	0.63

To help with the interpretation of the data from Table 2, a three-dimensional plot of one hundred randomly selected pixels from shaded frames are displayed in Figure 4. Only twenty randomly selected pixels were plotted from the average frame.

**Figure 4. Randomly Selected Pixel Values for the Blue Frames**

Green Background Analysis

The green background is analyzed next. Figure 5 shows the average green background for the first 42 frames and a typical shaded green background. Frames 43 and higher contain shaded pixels and are infeasible to include in the average background. The shaded frame is noticeable darker than the average green background.

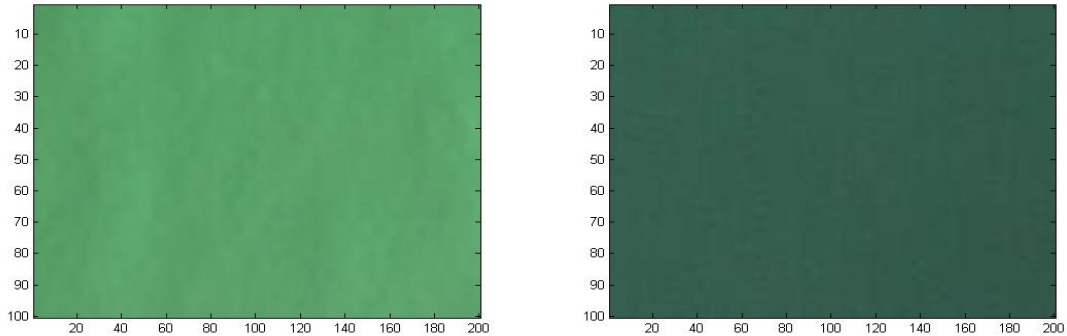


Figure 5. Green Average Background and Typical Shaded Frame

Figure 6 illustrates the average intensities of the RGB components of the average green frame and a typical shaded green frame. The green dimension is the most intense since the background is green. In contrast to the blue test data, the green material used was not as purely green as the blue background. The average intensities of the shaded frame are darkened due to the effect of shadow. The green component remains the most intense.

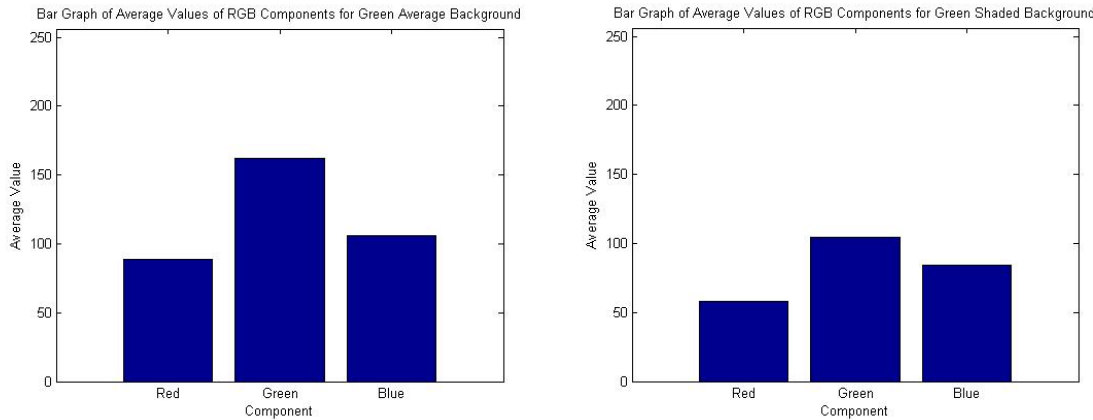


Figure 6. Intensities of Average Green Frame and Typical Shaded Green Frame

Table 3 is a representation of ten randomly selected pixels taken from the average green frame and the shaded green frame. The means and standard deviations were derived from the entire population of pixels.

Table 2. Randomly Selected Pixel Values for Green Background

	Red Component		Green Component		Blue Component	
	No Shadow	Shadow	No Shadow	Shadow	No Shadow	Shadow
88	53	162	91	105	76	
87	56	158	97	103	81	
87	52	162	96	105	81	
85	54	159	97	103	80	
88	53	161	94	105	78	
85	53	161	94	103	78	
88	53	158	91	103	76	
88	54	165	98	106	81	
88	51	163	95	106	78	
87	54	162	98	105	81	
Mean	88.30	53.06	161.58	94.52	105.39	78.34
St. Dev.	0.26	0.96	0.49	1.48	0.39	1.26

Figure 7 illustrates data taken from collected green frame data. One hundred randomly chosen pixels from shaded green frames were plotted. Twenty pixel values were plotted from the average green frame.

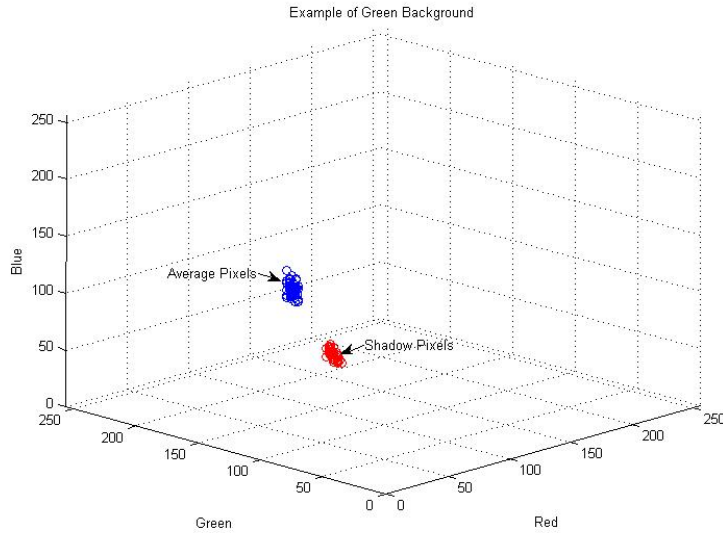


Figure 7. Randomly Selected Pixel Values for the Green Frames

Red Background Analysis

The final test data background color is red. The background is not one solid color due to small ripples in the construction paper background. The average background of the first 37 frames and a typical red shaded background are shown in Figure 8. Visually, the colors of the shaded background are more subdued.

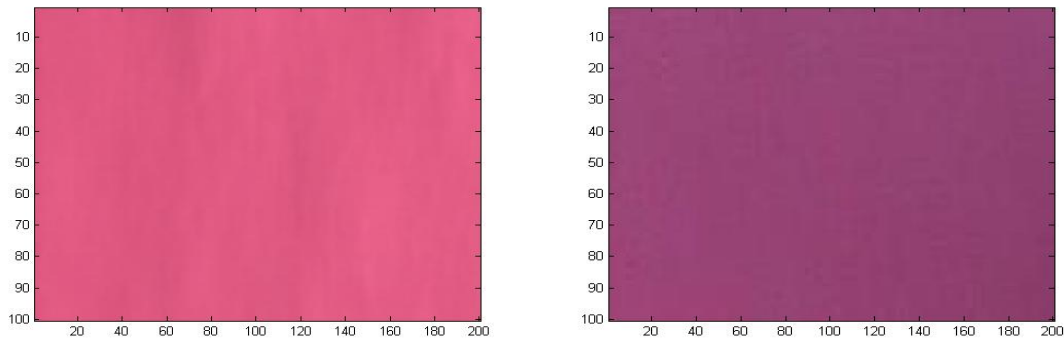


Figure 8. Red Average Background and Typical Shaded Frame

Figure 9 displays the average RGB intensities of the average red frame and typical shaded red frame. In this case, the red component has the highest intensity followed by the blue. The green component is the least intense due to the color of the construction paper. The green and red components are affected more by shadow than the blue component.

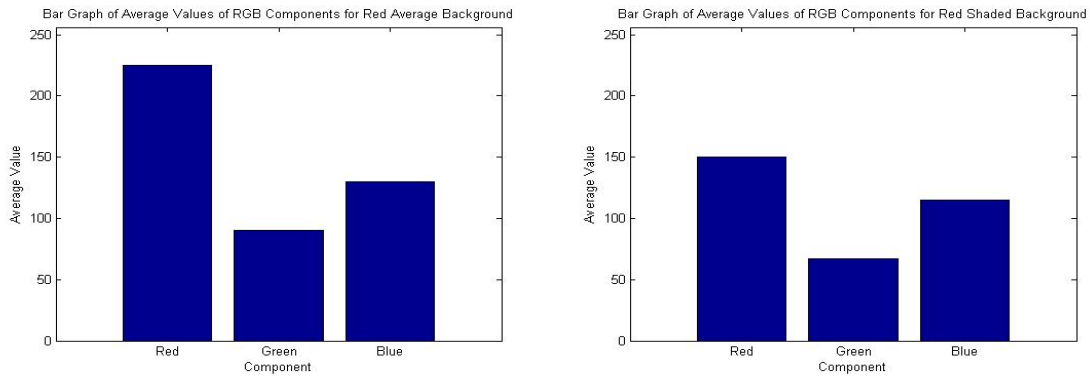


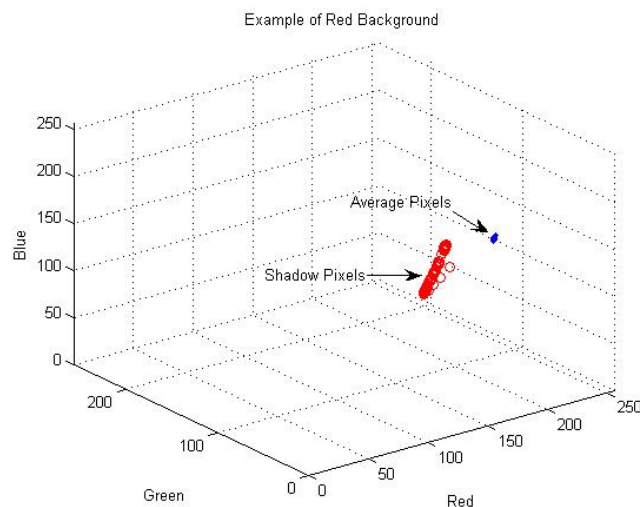
Figure 9. Intensities of Average Red Frame and Typical Shaded Red Frame

Table 3 is a random representation of ten pixels taken from the average frame and the shaded red frames. The mean and standard deviation derived from the entire population of pixels is also located in the table.

Table 3. Randomly Selected Pixel Values for the Red Frames

	Red Component		Green Component		Blue Component	
	No Shadow	Shadow	No Shadow	Shadow	No Shadow	Shadow
228	140	93	63	134	107	
227	144	93	65	133	110	
228	143	92	64	133	111	
223	147	90	64	130	110	
220	144	86	61	126	107	
229	146	93	67	134	114	
225	146	91	64	131	112	
226	147	91	65	131	113	
226	148	92	64	132	114	
226	148	91	66	132	114	
Mean	224.70	150.36	90.24	66.83	130.57	114.95
St. Dev.	0.76	0.96	0.47	0.67	0.70	0.92

In order to better visualize this data, Figure 10 is a three-dimensional graph of one hundred randomly chosen points from a shaded red background frame and twenty points from the average sunlit frame.

**Figure 10. Randomly Selected Pixel Values for the Red Frames**

Analysis of All Test Data

The data in all of the three-dimensional plots show a distinct relationship between the shaded pixel values and the average background pixel values. As a shadow is applied to a pixel, the corresponding RGB values of that pixel decrease. The observed amount of decrease is dependent on the individual RGB component. The blue component, in all three test cases, decreased less substantially than the red and green components. Intuitively the darkest a pixel value of a shadow can be is the value associated with the color black, which is represented with [0,0,0] in the RGB dimensional space. With the two ends of the major axis being the origin and the pixel value of the average background, and with an intermediate set of points representing the shaded pixels, the equation for an ellipsoid encompassing these intermediate set of shaded pixels can be derived. This is the basis of the rejection region utilized in the hypothesis test for this thesis.

In order to build the ellipsoidal rejection region, the parameters for an ellipsoid need to be solved for. Six parameters are needed to define a unique ellipsoid. These parameters are the coordinates of the center point and the lengths of the major and two minor axes. The ellipsoid equation is:

$$\left(\frac{x-u_1}{a}\right)^2 + \left(\frac{y-u_2}{b}\right)^2 + \left(\frac{z-u_3}{c}\right)^2 = 1 \quad (1)$$

In order for the rejection region of the hypothesis test to be employed without human intervention, the parameters for the ellipsoid need to be derived from the pixel values of the average background. The u variables correspond to the coordinates of the

center point of the ellipsoid. Since the ends of the major axis are the average background pixel value and the origin, the center point of the ellipse is the midpoint of the line formed by these points. The major axis of the ellipsoid, a , is the length of the line segment from the origin to the value of the pixel in the average photo which will be referred to as the ellipsoid centerline. The last two variables, b and c , are derived using the values of the shadow pixels in the test data. To find the two minor axes lengths, lengths that are hereafter termed the height and width of the ellipsoid, test data frames will be analyzed. Examining the distance of the values of the shadow pixels from a line created by average background pixel values and the origin reveals the distribution of the parameters of the ellipsoid. Figure 11 displays each RGB histogram of all of the three-dimensional distances of the shaded pixels to the ellipsoid centerline.

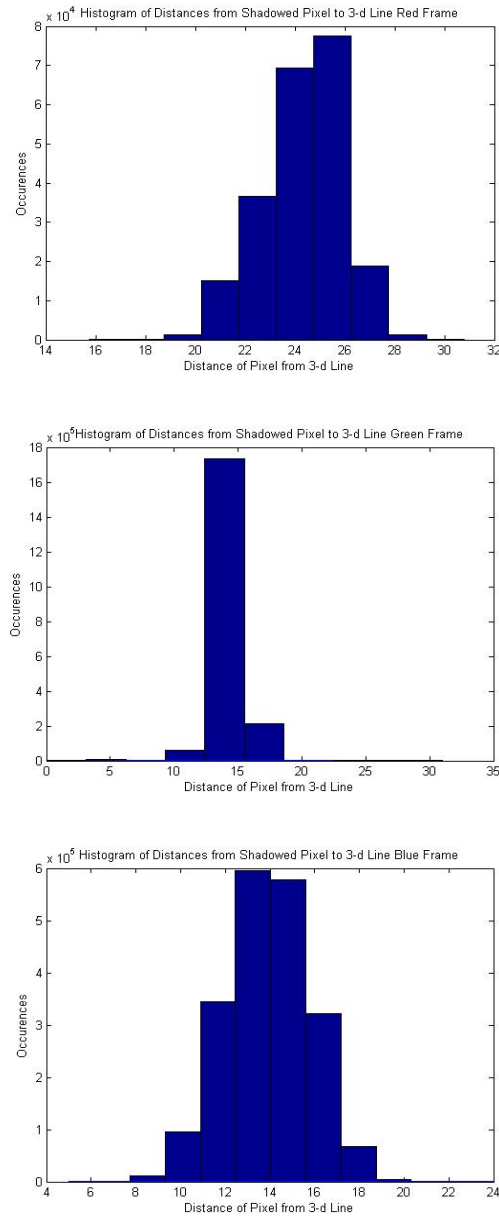


Figure 11. RGB Histograms of Distances of Shaded Pixels to Centerline

The three-dimensional distances of the shaded pixels to the ellipsoid centerline reveal shadow pixel distances but not where the pixels are located in relation to the centerline. Analyzing the two dimensional combinations of each RGB test frame would

reveal more insight into the orientation of the shaded pixel values in relation to the centerline.

The parameters of the ellipsoid need to be derived from the two-dimensional projected linear distances of the shaded pixel values to the mid-point of the line created by the average background pixels and the origin (centerline). There are three two-dimensional cases to discuss. The red/blue, green/blue and red/green components of the pixel values describe all combinations of three-dimensional representations.

The means and standard deviations of the two-dimensional distances of the shadow pixel values in relation to the ellipsoid centerline are in Table 4. The data was derived running the DistanceValues MATLAB algorithm in Appendix A. Analyzing Table 4 reveals that the blue component of the shadow pixels is responsible for the largest distances. Therefore, the ellipsoid height, corresponding to the blue axis, will be derived from combinations of blue/green or red/blue. The width of the ellipsoid will come from the combination of red/green components.

Table 4. Two-Dimensional Distances of Shadow Pixels to Ellipsoid Centerline

	Red Frame		Green Frame		Blue Frame	
	Mean	Std	Mean	Std	Mean	Std
Red/Blue	22.1125	2.0074	9.6296	1.5538	12.2105	1.8484
Blue/Green	10.6215	0.7989	13.9437	1.4901	10.3804	1.3814
Red/Green	4.4053	1.7505	1.6141	1.3314	2.6216	1.6968

The distances recorded in Table 4 were recorded at varying distances along the ellipsoid centerline. The two minor axes of the test ellipsoid can be thought of as emanating from the center of the ellipsoid. In order to get a shaded pixel distance from the center point of the ellipsoid, a three-dimensional line is projected from the average

background pixel value through the shaded pixel value, referred to as a shadow line. The tangent of the angle between the two lines is calculated. Taking the tangent of the angle and the distance from the average background pixel values to the center point of the ellipsoid reveals the orthogonal distance of the center point of the ellipsoid to the projected shadow line. Figures 12 through 14 display the concept discussed.

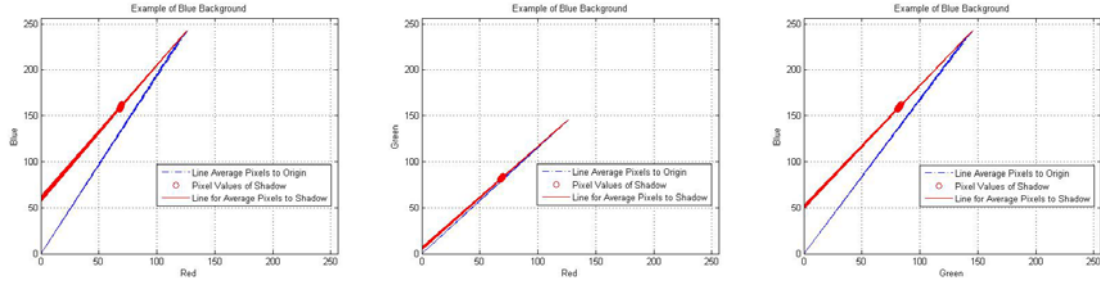


Figure 12. 2D Plots of Projected Shadow Lines of Blue Background

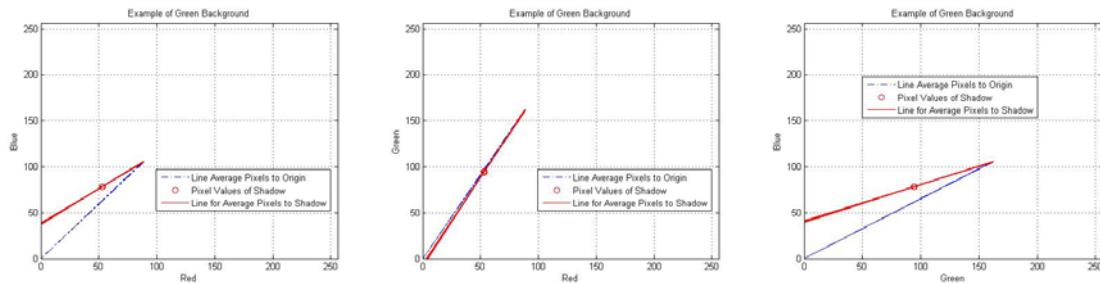


Figure 13. 2D Plots of Projected Shadow Lines of Green Background

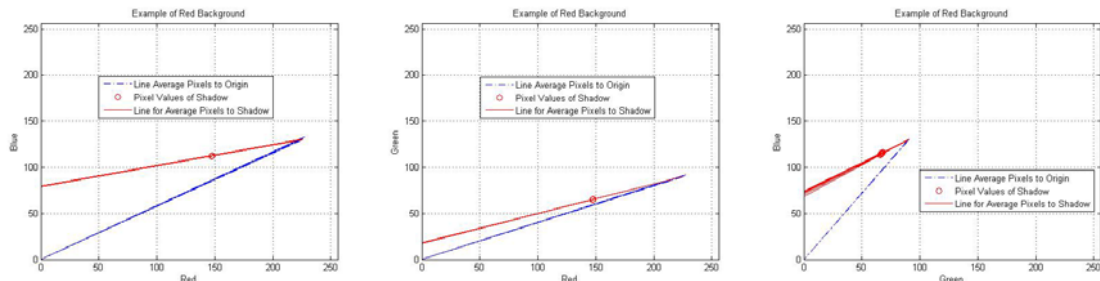


Figure 14. 2D Plots of Projected Shadow Lines of Red Background

The distances of the projected shadow line to the center of the ellipsoid and the charts in Figures 12 through 14 were created in the MATLAB program DistanceProjectedValues contained in Appendix A. To encapsulate the maximum amount of shadow pixels an upper 95% confidence interval of distances from the ellipsoid center point to the projected shadow line is utilized. Table 5 shows the average distances of the first ten frames of shadow pixels from the center point of the ellipsoid. Table 6 illustrates the upper 95% confidence intervals of all data collected. The information presented in Table 6 was output from the MATLAB program Confid in Appendix A.

Table 5. Average Distances of First Ten Shaded Frames

Red Frame			Green Frame			Blue Frame		
Red/Gr	Red/Bl	Blue/Gr	Red/Gr	Red/Bl	Blue/Gr	Red/Gr	Red/Bl	Blue/Gr
8.28	37.21	13.47	1.72	20.60	18.37	2.35	11.53	9.92
8.63	38.14	12.96	1.72	20.65	18.41	1.80	11.27	10.20
8.13	36.90	13.55	1.61	20.88	18.47	1.91	11.33	10.16
8.53	37.91	12.16	1.68	20.91	18.56	1.42	11.27	10.57
8.40	37.78	13.13	1.67	20.45	18.22	1.84	11.46	10.36
8.42	38.60	12.15	1.47	20.83	18.31	1.88	11.41	10.27
8.99	39.31	12.35	1.69	20.50	18.28	1.81	11.23	10.15
8.99	39.93	12.55	1.70	20.74	18.46	1.65	11.03	10.10
10.21	42.84	13.11	1.40	20.85	18.28	2.07	11.48	10.15
9.46	42.40	12.92	1.64	21.14	18.54	1.83	11.29	10.03

Table 6. Upper Confidence Intervals

	Red Frame	Green Frame	Blue Frame
	Mean	Mean	Mean
Red/Blue	43.2667	21.3211	13.2447
Red/Green	11.3852	2.2839	3.1505
Blue/Green	15.5642	18.7318	11.5069

Utilizing the distances for the RGB test data, an ellipsoid can be built to encompass the shadow pixels tailored to each particular frame. However, once the values are applied in different background color settings, the results are mixed. It is considered that the

ratios of the red, blue, and green components play an integral part in the values of shadow pixels.

The two-dimensional component combinations in each frame and the correlated upper confidence intervals are utilized to find their relationship. Three equations are constructed to account for the red/blue, red/green, and blue/green component combinations. Coefficients a and b are solved for the three combinations.

$$a \text{ (component value)} + b \text{ (component value)} = \text{Upper Confidence Interval} \quad (2)$$

The a and b coefficient for the red/blue components are [0.2467; 0.0584]. The coefficients for the blue/green components are [0.1294; 0.0242]. The red/green coefficients are [0.0783; 0.0512]. When an average background pixel value is introduced to the shadow removal algorithm, the respective pixel values of the color combinations are multiplied by their components and the larger of the two values is set to the height of the ellipsoid test region. With these coefficients, the parameter for the width minor axis can be determined. An example of a typical ellipsoid for testing can be seen in Figure 15. The height of the ellipsoid was set to ten and the width was set to five to illustrate that the height of the ellipsoid is greater than the width.

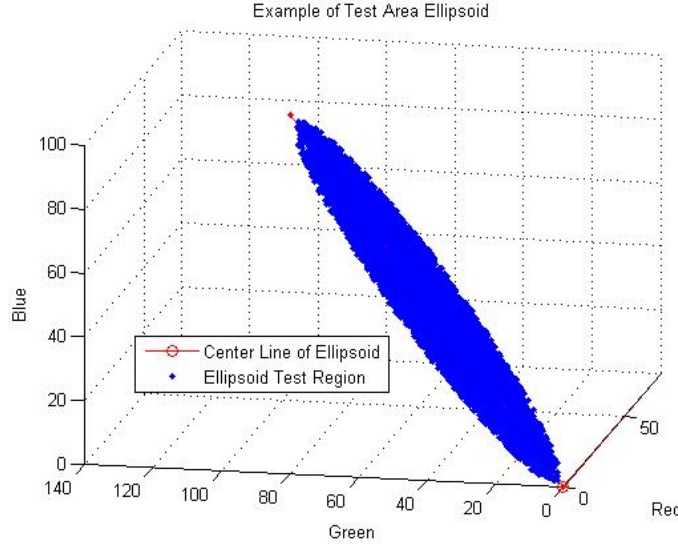


Figure 15. Example of Ellipsoid Test Region

The height and width of the critical region have been derived. In contrast the orientation of the critical region is vital to proper implementation. In order to orient the critical region, Euler angles and rotation matrices were employed. The ellipsoid equation is changed to matrix form to aid in the use of rotation matrices. Equation 3 illustrated the ellipsoid equation in matrix form. Equations 4 and 5 are the representations of the parameters of Equation 3. The x and u in Equation 4 are vectors of the three-dimensional components. The matrices in Equation 6 are the rotation matrices utilized to position the test region. Equation 7 is the completed rotation matrix. The order of the rotation matrices is important. Equation 8 is the final matrix form of the ellipsoid critical region with rotation matrices incorporated.

$$X^T V X = 1 \quad (3)$$

$$X = ((x) - (u)) \quad (4)$$

$$V = \begin{pmatrix} 1/a^2 & 0 & 0 \\ 0 & 1/b^2 & 0 \\ 0 & 0 & 1/c^2 \end{pmatrix} \quad (5)$$

$$R_y = \begin{pmatrix} \cos \theta & 0 & \sin \theta \\ 0 & 1 & 0 \\ -\sin \theta & 0 & \cos \theta \end{pmatrix} \quad (6)$$

$$R_z = \begin{pmatrix} \cos \theta & \sin \theta & 0 \\ -\sin \theta & \cos \theta & 0 \\ 0 & 0 & 1 \end{pmatrix}$$

$$R = R_y R_z \quad (7)$$

$$X^T R^T V R X = 1 \quad (8)$$

The rotation matrices are derived from data taken from the endpoint of the ellipsoid. A rotation about the blue axis is accomplished followed by a rotation on the green axis in order to orient the major axis of the ellipsoid along the line segment defined by the origin and the average pixel values. Figure 16 illustrates the procedure. The line parallel to the red axis is the start line, which represents the original line before rotation. The angle between the start line and the line in the red/green plane is calculated. The sine and the cosine of the angle is inserted R_y . Next, the angle between the line in the red/green plane and the center of the ellipsoid is calculated. In order to make this next transformation, only the sine of the angle is utilized and the cosine of the angle is set to 1. They are utilized in the R_z transformation matrix.

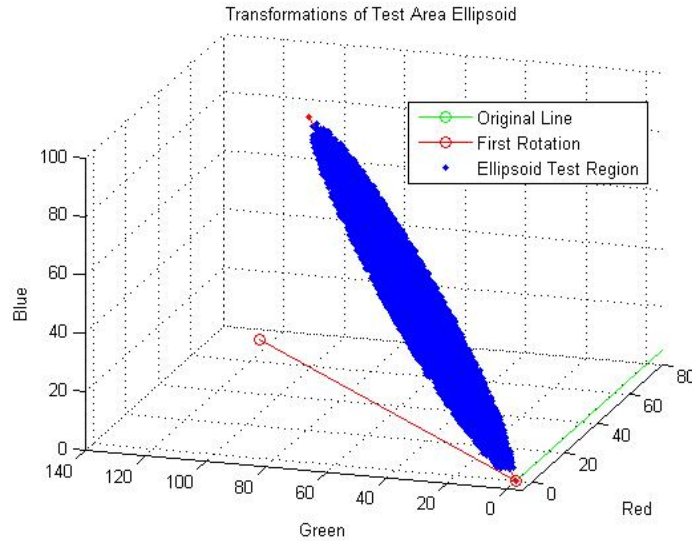


Figure 16. Representation of Transformations of Ellipsoid Test Region

Implementation

Having derived the equations to build the ellipsoidal critical region, utilization of the test on the solid colored test data was performed. Utilizing the ellipsoid rejection region, over 90 percent of the shadow pixels were removed from the blue background. Approximately 95 percent of the shadow pixel values in the green background were detected. The shadow pixels in the red background were detected 99 percent of the time. The percentages were not 100 percent due to the values of shadow pixels in three-dimensions. For example, if all three RGB values were outside of the 95 percent confidence interval of the critical region they would not get detected as a shadow pixel. The purpose of the algorithm is to eliminate a high percentage of shaded pixels. Although the results were reasonable, the program does allow for the tightening of parameters to ensure that objects are not removed that need to be studied. These solid

colored backgrounds were merely used to test the developed methodology in preparation for its use on gait data (Samler, 2006:60).

The true test of the algorithm comes from the removal of shadow without compromising the integrity of the rest of the image. As a point of reference for the rest of the discussion of results, the background subtraction method employed by Samler resulted in silhouettes in Figure 17 (Samler, 2006:60).



Figure 17. Images Derived from Background Subtraction

Frames 55, 56, and 57 of a single subject from the gait data were selected due to the position of the subject crossing the field of view. The subject is in full view of the camera. The binary silhouettes in Figure 18 represent an image with a significant amount of noise. There are several MATLAB filters that can help remove much of this noise. Unfortunately, the filters are ineffective at removing the shadow. The developed methodology of shadow removal via the ellipsoid test is utilized on the same three images and then the background subtraction algorithm is run. The results are in Figure 18.



Figure 18. Images After Ellipsoid Test and Background Subtraction

The noise in the three frames is slightly reduced. Of significance is the fact that the area around the subjects feet covered in shadow now appears shadow-free, albeit still noisy. In addition, there are portions of the silhouette that have been removed. Data of an individual is lost when a pixel value is in the critical region. This happens when an individual's clothing resembles that of the average background pixel value. Once a segment of the silhouette has been removed, that data of an individual is lost. If the data lost are interior points, a fill command may rectify the problem. However, if the pixels lost are boundary pixels on the silhouette, the size and shape will be altered. Depending on the amount of data lost, this process can significantly or minutely effect future calculations derived from output silhouettes.

MATLAB contains built-in functions to help enhance image quality. Utilizing the MATLAB built-in filter, medfilt2, the noise can be removed while maintaining the integrity of the silhouette. The medfilt2 filter takes the integer value of a determined neighborhood and returns the integer median value. Figure 19 was derived utilizing a 20 by 20 neighborhood.



Figure 19. Images After Ellipsoid Test and Background Subtraction with Filter

The image is still in need of certain corrections. The hole in the torso area was an error. This was due to the color of the subject's shorts. The color of the subject's shorts closely resembled the average background and the shadow produced by the outstretched arm on the shorts created pixel values residing in the ellipsoidal region. Since the missing data is a hole in the silhouette, another MATLAB function can be employed to handle errors of this type. The command imfill fills in holes in binary objects. Figure 20 is the representation of the same three silhouettes after the imfill command has been enacted.



Figure 20. Silhouette with Holes Filled

Summary

The effect of shadow on different combinations of colors can be mathematically represented. With this mathematical representation, the shadow pixels that belong to a corresponding color may be isolated and removed. The RGB test frames analyzed in this chapter aided in the derivation of an equation applied to an unrelated set of gait data that achieved shadow removal. The shadow of an individual can be removed without overly compromising the integrity of the subject walking across the field.

V. Conclusions and Recommendations

Chapter Overview

This chapter presents conclusions derived from results obtained in this thesis. In addition, future of research associated with the type of algorithm employed in this thesis will be suggested.

Conclusions of Research

This thesis presents a novel way to produce the binary silhouette of an individual free from the effects of shading. The developed algorithm seeks to eliminate shadow from images prior to the utilization of another algorithm that seeks to create a binary silhouette from a subject moving across the frame.

It is the contention of this thesis that the methodology presented accounts for differently colored backgrounds. The ellipsoidal critical region employed presents an attempt to remove pixels that are the same color as the average background pixel, though darker, and neglect data that is not related to the color of the background, which is likely an individual moving across the background. The algorithm allows for the removal of a large percentage of shaded colors.

The research question asked whether it is possible to remove shadow from a video feed without compromising the integrity of objects to be observed. The algorithm derived showed that it is possible to remove shadow from a video feed without losing a large amount of pertinent data. Furthermore, if small portions of the data associated with the individual are misclassified, smoothing and filling algorithms aid in the accurate rendering of a binary silhouette.

Recommendations for Future Research

This research is a small step toward the overachieving goal of realizing gait recognition as a feasible biometric. There are still avenues to be researched in the realm of shadow removal and the usage of the binary silhouettes.

The control was a single subject walking perpendicular to a video camera. This is a rather stringent setting. Variables such as plants or moving objects will add an amount of noise not handled by the shadow removal and background subtraction algorithms. The addition of multiple subjects in the frame to be tested would rest in multiple silhouettes. The multiple silhouettes would need to be manually separated by researchers to complete an analysis. Also, if two subjects were walking together, the algorithms would create a single indistinguishable silhouette.

In addition, if the camera is not stationary, the use of an average background becomes meaningless. There are two cases of camera movement that need further research. The camera could be oscillating left to right from a fixed location. The camera could be moving due to outside influences like wind or a person may be holding the camera.

Furthermore, the speed and space needed by an algorithm is of particular importance. The shadow removal and background subtraction algorithms test every pixel in every frame. With video data incorporating higher pixel counts, the algorithm will take longer to achieve a result and the size of stored average background will increase. The test area could be scaled down to only include the individual in a frame.

The use of the binary silhouettes will allow researchers to extract usable information concerning a subject being analyzed. With the proper algorithms, a subject's height, weight, gender could be determined.

There are a multitude of covariates that the shadow removal and background subtraction algorithm do not account for. For example, a subject could carry a briefcase to obstruct the rendering of a binary silhouette. Moreover, the wearing a dress or flowing robes would obstruct the legs of a subject. Further research is also needed to test the effect of subjects carrying heavy loads. There are several avenues open for further research.

Summary

This chapter discussed recommendations for future research and the conclusions of the research. The research shows that it is possible to remove the shadow of an individual without losing data needed for further processing. In addition, it has been demonstrated that a binary silhouette can be rendered automatically from only the input of test frames. There is still a multitude of research to be accomplished in the field of gait recognition. This thesis moves towards the ultimate goal of an automated gait recognition algorithm.

Appendix A. MATLAB Algorithms

Function: Load Video

```
function LoadVideo
%The program loads video from a camera into a computer
clear
clc
close all

%demo('toolbox','image processing')
imaqInfo = imaqhwinfo
% contains information about the image acquisition adaptors available
on the system
imaqInfo.InstalledAdaptors
WinInfo = imaqhwinfo('winvideo')
vid = videoinput('winvideo',1);
set(vid, 'FramesPerTrigger',200)

start(vid)
wait(vid)
[f, t] = getdata(vid);
```

Function: Write Multiple Images

```
function Writemulti(start,stop,x,y,w,h)
%Write multiple images to file

for count = start:stop,
    red = g(:,:,:,:count); %assignment
    filename = (['red',num2str(count),'.jpg']);%creates file
    imwrite( red, filename );%writes file
end
```

Function: Crop Images

```
function [I,rsmall] = Crop(start,stop,x,y,w,h)
%Will grab a specified range of pixels and save them to file%
%start(1) First frame of no shadow
%stop(1) Last frame before shadow
%x coordinate of left of box
%y coordinate of top of box
%w width of box
%h height of box

for i=start(1):stop(1),
    I = imread(['C:\Documents and Settings\Owner\Desktop\Thesis\' 
    sprintf('red%i.jpg',i)]);
    rsmall = imcrop(I,[x y w h]);
    %removes croppped section from image
    filename = (['rsmall',num2str(i-start(1)+1),'.jpg']); %creates
    filename connected to each individual jpg
    imwrite(rsmall, filename); %writes cropped file to file
end
```

Function: Three-Dimensional Data Plots

```
function DataPlots
%3d plot of pixel values

start(1)= 1; %First frame of no shadow
stop(1) = 34; %Last frame of no shadow

start(2) = 45;%First frame with shadow
stop(2) = 150;%Last frame

for i=start(1):stop(1),
    I(:,:,:,:i-start(1)+1) = imread(['C:\Documents and
    Settings\Owner\Desktop\Thesis\' sprintf('small%i.jpg',i)]);
end

for i=start(1):stop(1),
    figure=plot3(mean(mean(I(:,:,1,i))),mean(mean(I(:,:,2,i))),mean(m
    ean(I(:,:,3,i))),'.');%3-d plot of first vs last frame
    hold on
end

for i=start(2):stop(2),
    I(:,:,:,:i) = imread(['C:\Documents and
    Settings\Owner\Desktop\Thesis\' sprintf('small%i.jpg',i)]);
end

for i=start(2):stop(2),
    figure=plot3(mean(mean(I(:,:,1,i))),mean(mean(I(:,:,2,i))),mean(m
    ean(I(:,:,3,i))),'ro');%3-d plot of first vs last frame
    hold on
    grid on
    axis([0 256 0 256 0 256])
    xlabel('Red')
    ylabel('Green')
    zlabel('Blue')
    title('Example of blue background')
end

hold off
```

Function: Display Average RGB Intensities

```
function [A,photoavg] = RGBBackground(start,stop);(Samler, 2006:60)
% Reads jpegs into matlab, then finds an avg RGB intensity for
% background, gives% back an average background picture. Also
% gives the background picture in subplots of the Red, Green
% and Blue intensities.

close all

for i=start(1):stop(1),
    A(i-start(1)+1,:,:,:)=imread(['C:\Documents and
    Settings\Owner\Desktop\Thesis\' sprintf('gsmall%i.jpg',i)]);
end

s = size(A,4); %Displays average photo as image
photoavg=mean(A);
photoavg = squeeze(photoavg);
image(uint8(photoavg));

figure %displays 3 intensities 1-red 2-green 3-blue
colormap(gray(256));
subplot(3,1,1);image(photoavg(:,:,1))
subplot(3,1,2);image(photoavg(:,:,2))
subplot(3,1,3);image(photoavg(:,:,3))
```

Function: Computation of Three-Dimensional Distances

```
function DistanceValues;
%Computes distances from a point to a 3d vector

start(1)= 1; %First frame of no shadow
stop(1) = 34; %Last frame of no shadow

start(2) = 55;
stop(2) = 150;

for i=start(1):stop(1),
    A(i-start(1)+1,:,:,:) = imread(['C:\Documents and
    Settings\Owner\Desktop\Thesis\' sprintf('rsmall%i.jpg',i)]);
end
photoavg = (mean(A)); %Average photo
A = squeeze(photoavg);%Takes left column vector away
A=int16(A);

for i=start(2):stop(2),
    I(:,:, :,i) = imread(['C:\Documents and
    Settings\Owner\Desktop\Thesis\' sprintf('rsmall%i.jpg',i)]);
end

for n = 1:200; %cycle through
    for m = 1:100; %cycle through
        for i=start(2):stop(2),
            d = double(A(m,n,1));
            e = double(A(m,n,2));
            f = double(A(m,n,3));
            a = double(I(m,n,1,i));
            b = double(I(m,n,2,i));
            c = double(I(m,n,3,i));
            d1(i-start(2)+1)=sqrt((a-d)^2 + (b-e)^2 + (c-
            f)^2)*sin(acos((a-d)*d + (b-e)*e+(c-f)*f)/(sqrt((a-d)^2 +
            (b-e)^2 + (c-f)^2)*sqrt(d^2+e^2+f^2)) );
        end
    end
end
avg = mean(d1);
s = std(d1)
```

Function: Computation of Projected Three-Dimensional Distances

```
function DistanceProjectedValues;
%Computes a projected shadow line
%Computes the 3d distance of point to shadow line
start(1)= 1; %First frame of no shadow
stop(1) = 34; %Last frame of no shadow

start(2) = 116;
stop(2) = 150;

for i=start(1):stop(1),
    P(:,:,:,:i-start(1)+1) = imread(['C:\Documents and
    Settings\Owner\Desktop\Thesis\' sprintf('small%i.jpg',i)]);
end

for i=start(1):stop(1),
    V1=[mean(mean(P(:,:,1,i)));0]];%average color of background
    V2=[mean(mean(P(:,:,2,i)));0];
    A=plot(V1,V2,'.-');%plot average color pixel to origin
    hold on
    S(:,i)=[V1(1);V2(1)];
    m1(i)=(V2(1)/V1(1));%slope of line
end
for i=start(2):stop(2),
    I(:,:,:,:i-start(2)+1) = imread(['C:\Documents and
    Settings\Owner\Desktop\Thesis\' sprintf('small%i.jpg',i)]);
end
for i=1:(stop(2)-start(2)),
    V3=[mean(mean(I(:,:,1,i)))];%average color of shadow
    V4=[mean(mean(I(:,:,2,i)))];;
    m2=(V4-S(2,i))/(V3-S(1,i));%slope of line from average pixel no
    shadow vs shadow
    tatheta(i)=-(m2-m1(i))/(1+m1(i)*m2);%tangent of angle between lines
    b=V4-V3*(m2);%y intercept
    xo=b/(-m2);%x intercept
    opp(i)= tatheta(i)*sqrt((S(1,i)/2)^2+(S(2,i)/2)^2);%distance
    between line at midpoint

    B=plot(V3,V4,'ro');%plot of shadow point
    C=plot([S(1,i);xo],[S(2,i);0],'-r');%plot of shadow line
    legend( [ A , B , C ] , 'Line Average Pixels to Origin', 'Pixel
    Values of Shadow', 'Line for Average Pixels to Shadow' );
    grid on
    axis([0 256 0 256])
    xlabel('Red')
    ylabel('Green')

    title('Example of Blue Background')
end

hold off
q=mean(opp);%mean distance
r=std(opp);%std distance
ci=abs(q)+1.96*sqrt(abs(r/q));%upper confidence interval
```

Function: Shadow Removal Algorithm

```
function ShadowTest;
%Test to remove shadow from test images
close all
start(1)=1;
stop(1)=36;

for i=start(1):stop(1),
    A(i-start(1)+1,:,:,:) = imread(['C:\Documents and
    Settings\Owner\Desktop\Thesis\' sprintf('rsmall%i.jpg',i)]);
end

start=55;
stop=60;
for i=start:stop,
    P(:,:,i-start+1)=imread(['C:\Documents and
    Settings\Owner\Desktop\Thesis\' sprintf('rsmall%i.jpg',i)]);
%Image is stored as a three-dimensional (m-by-n-by-3) array of integers
in the range [0, 255] (uint8)
end
photoavg = (mean(A)); %average picture
photoavg = double((squeeze(photoavg))); %changes 4d to 3d

tt= zeros(1,(stop-start+1)); %Preload Variable

for m = 1:100;%cycle through 720
    for n =1:200 ; %cycle through 480
        c = [(photoavg(m,n,1));(photoavg(m,n,2));(photoavg(m,n,3))];
        %Ellipse end point
        z1=c(1)/sqrt(c(1)^2+c(2)^2);%red and green
        z2=c(2)/sqrt(c(1)^2+c(2)^2);%cos angle red and blue shift
        Rz=[[z1 -z2 0],[z2 z1 0],[0 0 1]]; %rotation matrix about z

        for i=start:stop,
            d = double(P(m,n,1,i-start+1));
            e = double(P(m,n,2,i-start+1));
            f = double(P(m,n,3,i-start+1));
            g = [0.0951;0.0486];%Coefficients for green red
            h = [0.0792;0.0955];%coefficients for blue red
            gp=[d,e]*g; %output for ellipsoid width
            bp=[e,f]*h; %output for ellipsoid height
            ah(m,n,i-start+1)=gp;
            bh(m,n,i-start+1)=bp;
            points = [d;e;f]; %Points in ellipse
            cpoints = ((c+[0;0;bp/2])/2)- points;%Center ellipse
            g=[[0;0;0],[c+[-c(1)+sqrt(c(1)^2+c(2)^2+c(3)^2);-c(2);-
            c(3)]]];

            g=Rz'*g; %transform of line around z

            y=[1;c(3)/sqrt(c(1)^2+c(2)^2)];
            %cos =1 sin of angle between shifted line and

```

```

Ry=[[y(1) 0 -y(2)]',[0 1 0]',[y(2) 0 y(1)']];
%rotation matrix about y

R = Ry*Rz; %complete rotation matrix

j=sqrt(c(1)^2 + c(2)^2 + c(3)^2+1);%major axis of ellipsoid
if gp > 0;
    if bp > 0;
        V=[[1/(j/1.9)^2 0 0],[0 1/(gp)^2 0],[0 0
        1/(bp)^2]'];%Length axes
    end
end
ell=sum((R*cpoints).*(V*R*cpoints));
%Matrix ellipse equation
ch(m,n,i-start+1)=ell; %Matrix ellipse equation
if ell < 1,
    tt(1,i-start+1)=tt(1,i-start+1)+1;
    for p=1:3
        P(m,n,p,i-start+1)=(photoavg(m,n,p));
        %Replaces a pixel in an image with the average for
        that pixel
    end
end
end
end
end

```

Function: Computation of Upper Confidence Intervals

```
function Confid;
%Compute confidence intervals of
%distances of shadow line to a point
clc
clear
start(1)= 1; %First frame of no shadow
stop(1) = 34; %Last frame of no shadow

start(2) = 116;
stop(2) = 150;

for i=start(1):stop(1),
    P(i-start(1)+1,:,:,:) = imread(['C:\Documents and
    Settings\Owner\Desktop\Thesis\' sprintf('small%i.jpg',i)]);
end
photoavg = (mean(P)); %average picture
photoavg = double((squeeze(photoavg))); %changes 4d to 3d
for i=start(2):stop(2),
    I(:,:,:,:i-start(2)+1) = imread(['C:\Documents and
    Settings\Owner\Desktop\Thesis\' sprintf('small%i.jpg',i)]);
end

for i=1:(stop(2)-start(2)),
    for m = 1:100;%cycle through 720
        for n = 1:200; %cycle through 480
            V = [photoavg(m,n,1),(photoavg(m,n,2)),(photoavg(m,n,3))];
            %Ellipse end point
            m1 = (V(3)/V(1));%slope of line
            V1 = [double(I(m,n,1,i))];%average color of shadow
            V2 = [double(I(m,n,2,i))];
            V3 = [double(I(m,n,3,i))];
            m2=(V(3)-V3)/(V(1)-V1);
            %slope of line from average pixel no shadow vs shadow
            tatheta=(m2-m1)/(1+m1*m2);%tangent of angle between lines

            opp(m,n,i)= -tatheta*sqrt(((V(1))/2)^2+((V(2))/2)^2);
            %distance between line at midpoint
        end
    end
end

q=squeeze(mean(squeeze(mean(opp))));%mean distance
r=std(q);%std distance
for i=1:(stop(2)-start(2)),
    ci(i)=abs(q(i))+1.96*sqrt(abs(r*1/q(i)));%upper confidence interval
end
max(ci)
```

Function: Computation of Coefficients for Shadow Removal Algorithm

```
function Coeff;
%Compute coefficients used in Test.m

close all
start(1)=1;
stop(1)=36;

for i=start(1):stop(1),
    A(i-start(1)+1,:,:,:) = imread(['C:\Documents and
    Settings\Owner\Desktop\Thesis\' sprintf('small%i.jpg',i)]);
end
photoavgB = (mean(A)); %average picture
photoavgB = double((squeeze(photoavgB))); %changes 4d to 3d

for i=start(1):stop(1),
    A(i-start(1)+1,:,:,:) = imread(['C:\Documents and
    Settings\Owner\Desktop\Thesis\' sprintf('rsmall%i.jpg',i)]);
end
photoavgR = (mean(A)); %average picture
photoavgR = double((squeeze(photoavgR))); %changes 4d to 3d

for i=start(1):stop(1),
    A(i-start(1)+1,:,:,:) = imread(['C:\Documents and
    Settings\Owner\Desktop\Thesis\' sprintf('gsmall%i.jpg',i)]);
end
photoavgG = (mean(A)); %average picture
photoavgG = double((squeeze(photoavgG))); %changes 4d to 3d

T(1,:)=[mean(mean(photoavgG(:,:,1))),mean(mean(photoavgG(:,:,2))),mean(
mean(photoavgG(:,:,3))]];
T(2,:)=[mean(mean(photoavgR(:,:,1))),mean(mean(photoavgR(:,:,2))),mean(
mean(photoavgR(:,:,3))]];
T(3,:)=[mean(mean(photoavgB(:,:,1))),mean(mean(photoavgB(:,:,2))),mean(
mean(photoavgB(:,:,3))];

RB=[T(:,1),T(:,3)];
RG=[T(:,1),T(:,2)];
RB2 = [43.2667; 21.3211; 13.2447];
RG2 = [11.3852; 2.2839; 3.1505];
coefg=RB\RB2
coefB=RG\RG2
```

Function: Plot of Rotation of Ellipsoid

```
function RotationPlot;
%Displays the order and placement of a line after rotations
clear
n=500000;
c = [91;61;107]; %Ellipse end point
points = rand([3,n])*100; %Points in ellipse
cpoints = points - repmat((c+[0;0;0])/2,[1 n]);%Center ellipse

z1=c(1)/sqrt(c(1)^2+c(2)^2);%red and green
z2=c(2)/sqrt(c(1)^2+c(2)^2);

Rz=[[z1 -z2 0],[z2 z1 0],[0 0 1]]; %rotation matrix about z
g=[[0;0;0],[c+[-c(1)+sqrt(c(1)^2+c(2)^2+c(3)^2);-c(2);-c(3)]]];
%Line on xy plane
A=plot3([g(1,:)],[g(2,:)],[g(3,:)],'o-g');
%Plot Original Line
hold on
g=Rz'*g; %Transformation of line about z
%B=plot3([g(1,:)],[g(2,:)],[g(3,:)],'o-b');
%Line after transformation

y=[1;c(3)/sqrt(c(1)^2+c(2)^2)];
%Angle for y transformation leaving x alone
Ry=[[y(1) 0 -y(2)],[0 1 0],[y(2) 0 y(1)]]; %rotation matrix about y
R = Ry*Rz; %full rotation matrix
C=plot3([g(1,:)],[g(2,:)],[g(3,:)],'o-r');
%Line Trying to get
l=sqrt(c(1)^2+c(2)^2+c(3)^2)+2;%major axis of ellipsoid
V=[[1/((l+25)/2)^2 0 0],[0 1/(10)^2 0],[0 0 1/(18)^2]];%Length axes
ell=sum((R*cpoints).*(V*R*cpoints));
%Matrix ellipse equation
index = find(ell<2);

D=plot3(points(1,index),points(2,index),points(3,index),'.');
%3-d plot of first vs last frame
legend( [A ,C,D] , 'Original Line','First Rotation' , 'Ellipsoid Test
Region' );
grid on
axis([0 100 0 70 0 120])
xlabel('Red')
ylabel('Green')
zlabel('Blue')
title('Transformations of Test Area Ellipsoid')
plot3([0 c(1)],[0 c(2)],[0 c(3)],'.-r'); %Line Trying to get to

hold off
```

Function: Shadow Removal and Back Ground Subtraction

```
function Test;
%Removes shadow then runs background subtraction
close all
start(1)=1;
stop(1)=5;
start(2)=124;
stop(2)=128;

for i=start(1):stop(1),
    A(i-start(1)+1,:,:,:)=imread(['C:\Documents and
        Settings\Owner\Desktop\Thesis\Pass#1\' sprintf('frame%i.jpeg',i)]);
end

for i=start(2):stop(2),
    A(stop(1)+i-start(2)+1,:,:,:)=imread(['C:\Documents and
        Settings\Owner\Desktop\Thesis\Pass#1\' sprintf('frame%i.jpeg',i)]);
end

start=55;
stop=57;
for i=start:stop,
    P(:,:,i-start+1)=imread(['C:\Documents and
        Settings\Owner\Desktop\Thesis\Pass#1\' sprintf('frame%i.jpeg',i)]);
    %Image is stored as a three-dimensional (m-by-n-by-3) array of
    %integers in the range [0, 255] (uint8)
end
photoavg = (mean(A)); %average picture
photoavg = double((squeeze(photoavg))); %changes 4d to 3d

for m = 1:480;%cycle through 720
    for n =1:720 ; %cycle through 480
        c = [(photoavg(m,n,1));(photoavg(m,n,2));(photoavg(m,n,3))];
        %Ellipse end point
        z1=c(1)/sqrt(c(1)^2+c(2)^2);%red and green
        z2=c(2)/sqrt(c(1)^2+c(2)^2);%cos angle red and blue shift
        Rz=[[z1 -z2 0],[z2 z1 0],[0 0 1]]; %rotation matrix about z

        for i=start:stop,
            d = double(P(m,n,1,i-start+1));
            e = double(P(m,n,2,i-start+1));
            f = double(P(m,n,3,i-start+1));

            q = [0.0783;0.0512];%coefficients for green red
            h = [0.2467;0.0584];%Coefficients for blue red
            p = [0.1294;0.0242];%Coefficients for blue green
            gp=[d,e]*q; %output for ellipsoid width
            bp1=[d,f]*h; %output for ellipsoid height
            bp2=[e,f]*p; %output for ellipsoid height
            bp=max(bp1,bp2);
            ah(m,n,i-start+1)=gp;
            bh(m,n,i-start+1)=bp;
```

```

points = [d;e;f]; %Points in ellipse
cpoints = ((c+[0;0;bp/2])/2)- points;%Center ellipse
g=[[0;0;0],[c+[-c(1)+sqrt(c(1)^2+c(2)^2+c(3)^2);-c(2);-c(3)]]];

g=Rz'*g; %transform of line around z

y=[1;c(3)/sqrt(c(1)^2+c(2)^2)];%cos =1 sin of angle between
shifted line and

Ry=[[y(1) 0 -y(2)]',[0 1 0]',[y(2) 0 y(1)]]; %rotation
matrix about y

R = Ry*Rz; %complete rotation matrix

j=sqrt(c(1)^2 + c(2)^2 + c(3)^2+1);%major axis of ellipsoid
if gp > 0;
    if bp > 0;
        v=[[1/(j/1.9)^2 0 0]',[0 1/(gp/2)^2 0]',[0 0
        1/(bp/2)^2]'];%Length axes
    end
end
ell=sum((R*cpoints).*(V*R*cpoints));
%Matrix ellipse equation
ch(m,n,i-start+1)=ell; %Matrix ellipse equation
if ell < 1,
    for p=1:3
        P(m,n,p,i-start+1)=(photoavg(m,n,p));%Replaces a
        pixel in an image with the average for that pixel
    end
end
end
end
k = 5.2;%Standard Deviations(Samler, 2006:60)
for i=1:size(A,1);
    diffavg1(i,:,:,:,:) = squeeze(int16(A(i,:,:,:,:)) - int16(photoavg));
    %Used to help find variances of differences
end

Asize = prod(size(diffavg1(:,:,:,:,1)));
for i=1:3
    v(i)= var(reshape(diffavg1(:,:,:,:,i),Asize,1,1,1));
end

for i=1:size(P,4);
    I2=int16(photoavg)-int16(P(:,:,:,:,i));
    I(:,:,:,:,i)=(I2(:,:,:,:1).^2/(k*v(1))+I2(:,:,:,:2).^2/(k*v(2))+I2(:,:,:,:3).^2/(k
    *v(3))>1);
    I(:,:,:,:,i) = medfilt2(I(:,:,:,:,i),[20 20]);
    I(:,:,:,:,i) = imfill((I(:,:,:,:,1)),'holes');
end
figure
for i=1:size(P,4);
    subplot(1,3,i)%rows,columns,frames
    imshow(I(:,:,:,:,i))
end

```

Bibliography

“Biometrics.” Excerpt from Merriam-Webster online dictionary. N. pag. <http://www.merriam-webster.com/dictionary/biometrics>. 10 December 2007.

Boulgouris, Nikolas V., Konstantinos N. Platantinos, and Dimitrios Hatzinakos. “Gait Recognition Using Linear Time Normalization,” *Pattern Recognition*, 39: 969-979 (May 2006).

-----, and Zhiwei X. Chi. “Human Gait RecognitionBased on Matching of Body Components,” *Pattern Recognition*, 40: 1763-1770 (June 2007).

Bowden, R., T.A. Mitchell, and M. Sarhadi. “Non-Linear Statistical Models for the 3D Reconstruction of Human Pose and Motion from Monocular Image Sequences,” *Image and Vision Computing*, 18: 729-737 (2000).

Capozzo, Aurelio, and others. “Human Movement Analysis Using Stereophotogrammetry, Part I: Theoretical Background,” *Gait and Posture*, 21: 186-196 (2005).

Foster, Jeff P., Mark S. Nixon, and Adam Prugel-Bennett. “Automatic Gait Recognition Using Area-Based Metrics,” *Pattern Recognition Letters*, 24: 2489-2497 (October 2003).

“Gait.” Excerpt from online medical dictionary. N. pag. <http://medical-dictionary.thefreedictionary.com/gait>. 19 December 2007.

Herbison-Evans, Don. “Animated Cartoons by Computers Using Ellipsoids.” Unpublished Technical Report No. 94. University of Sydney, Sydney Australia, 1974. 14 February 2008 <http://www-staff.mcs.uts.edu.au/~don/pubs/cartoon.html>.

Lam, Toby H.W., Raymond S.T. Lee, and David Zhang. “Human Gait Recognition by the Fusion of Motion and Static Spatio-Temporal Templates,” *Pattern Recognition*, 40: 2563-2573 (September 2007).

Liu, Zongyi and Sudeep Sarkar. “Effect of Silhouette Quality on Hard Problems in Gait Recognition,” *IEEE Transactions on Systems, Man, and Cybernetics-Part B: Cybernetics*, 35: 170-183 (April 2005).

Phillips, Jonathon P., Patrick Grother, Sudeep Sarkar, Isidro Robledo, Patrick Grother, and Kevin Bowyer. “Baseline Results for the Challenge Problem of Human ID Using Gait Analysis,” *Proceedings of the Fifth IEEE International Conference on Automatic Face and Gesture Recognition*. 137. New York: IEEE Press, 2002.

Post, David C. "Gait Analysis Review." Excerpt from unpublished article.
<http://www.nd.edu/~dpost/IntSyst/report1.pdf>. 28 February 2006.

Samler, Jennifer J. *Statistical Approach to Background Subtraction for Production of High-Quality Silhouettes for Human Gait Recognition*. MS Thesis, AFIT/GAM/ENC/06-04. School of Systems and Logistics, Air Force Institute of Technology (AU), Wright-Patterson AFB OH, September 2006 (ADA456804).

Wang, J. M., Y.C. Chung, C.L. Chang, and S.W. Chen. "Shadow Detection and Removal for Traffic Images," *Proceedings of the 2004 IEEE International Conference on Networking, Sensing, and Control*. 649-654. New York: IEEE Press, 2004.

Vita

Second Lieutenant Brian D. Hockersmith was born in Fort Stewart, GA. He graduated Cocoa High School, Cocoa, FL in May 1994. He graduated from the University of West Florida in May 2006.

Lieutenant Hockersmith joined the Air Force in October 1996. His first enlisted assignment was Hurlburt Field, FL. Once finished with his Bachelor's Degree, he commissioned as an Officer in the Air Force. His first assignment as an officer was The Air Force Institute of Technology (AFIT) to pursue a Master of Science in Mathematics Degree.

REPORT DOCUMENTATION PAGE				<i>Form Approved OMB No. 074-0188</i>
<p>The public reporting burden for this collection of information is estimated to average 1 hour per response, including the time for reviewing instructions, searching existing data sources, gathering and maintaining the data needed, and completing and reviewing the collection of information. Send comments regarding this burden estimate or any other aspect of the collection of information, including suggestions for reducing this burden to Department of Defense, Washington Headquarters Services, Directorate for Information Operations and Reports (0704-0188), 1215 Jefferson Davis Highway, Suite 1204, Arlington, VA 22202-4302. Respondents should be aware that notwithstanding any other provision of law, no person shall be subject to an penalty for failing to comply with a collection of information if it does not display a currently valid OMB control number.</p> <p>PLEASE DO NOT RETURN YOUR FORM TO THE ABOVE ADDRESS.</p>				
1. REPORT DATE (DD-MM-YYYY) 03-19-2008	2. REPORT TYPE Master's Thesis			3. DATES COVERED (From – To) March 2007 – March 2008
4. TITLE AND SUBTITLE Statistical Removal of Shadow for Applications to Gait Recognition			5a. CONTRACT NUMBER	
			5b. GRANT NUMBER	
			5c. PROGRAM ELEMENT NUMBER	
6. AUTHOR(S) Hockersmith, Brian, Second Lieutenant, USAF			5d. PROJECT NUMBER	
			5e. TASK NUMBER	
			5f. WORK UNIT NUMBER	
7. PERFORMING ORGANIZATION NAMES(S) AND ADDRESS(S) Air Force Institute of Technology Graduate School of Engineering and Management (AFIT/EN) 2950 Hobson Way WPAFB OH 45433-7765			8. PERFORMING ORGANIZATION REPORT NUMBER AFIT/GAM/ENC/08-04	
9. SPONSORING/MONITORING AGENCY NAME(S) AND ADDRESS(ES) Intentionally left blank			10. SPONSOR/MONITOR'S ACRONYM(S)	
			11. SPONSOR/MONITOR'S REPORT NUMBER(S)	
12. DISTRIBUTION/AVAILABILITY STATEMENT APPROVED FOR PUBLIC RELEASE; DISTRIBUTION UNLIMITED				
13. SUPPLEMENTARY NOTES				
<p>14. ABSTRACT The purpose of this thesis is to mathematically remove the shadow of an individual on video. The removal of the shadow will aid in the rendering of higher quality binary silhouettes than previously allowed. These silhouettes will allow researchers studying gait recognition to work with silhouettes unhindered by unrelated data. The thesis begins with the analysis of videos of solid colored backgrounds. A formulation of the effect of shadow on specified colors will aid in the derivation of a hypothesis test to remove an individual's shadow. Video of an individual walking normally, perpendicular to the camera will be utilized to test the algorithm.</p> <p>First, the algorithm replaces shaded pixels, pixel values determined to be shadows, with corresponding pixels of an average background. A hypothesis test will be employed to determine if a pixel value is a shaded pixel. The rejection region for the hypothesis test will be determined from the pixel values of the frames containing a subject. Once the shaded pixels are replaced, the resulting frames will then be run through a background subtraction algorithm and filtered, resulting in a series of binary silhouettes. Researchers can then utilize the series of binary silhouettes to accomplish a gait recognition algorithm.</p>				
15. SUBJECT TERMS Silhouettes, Algorithms, Shadows, Detection				
16. SECURITY CLASSIFICATION OF:		17. LIMITATION OF ABSTRACT	18. NUMBER OF PAGES	19a. NAME OF RESPONSIBLE PERSON Samuel A. Wright, Maj., USAF
REPORT U	ABSTRACT U	c. THIS PAGE U	UU	19b. TELEPHONE NUMBER (Include area code) (937) 255-3636; ext. 4549 (samuel.wright@afit.edu)